



TM-1412
0427.000

MAGNETIC MEASUREMENTS OF THE CORRECTION AND ADJUSTMENT
MAGNETS OF THE MAIN RING

D. Trbojevic

July 1986



MAGNETIC MEASUREMENTS OF THE CORRECTION AND ADJUSTMENT MAGNETS OF THE MAIN RING

D.Trbojevic
July 1986

Correction magnets correct the field imperfections and alignment errors of the main quadrupoles and bend magnets. For reducing and controlling chromaticity there are 186 sextupoles and 78 octupoles, while for suppressing various resonances there are 12 normal and 18 skew sextupoles and 24 normal and 18 skew quadrupoles. Beam positions are individually controlled by 108 horizontal and 108 skew dipoles.

This report includes results of the all Main Ring correction and adjustment magnet harmonic measurements. The measurement principle and basic equations are described in Appendix 1.

1. SEXTUPOLE MAGNETS

Twelve normal sextupoles located at stations 28 and 35 are used to compensate for the third integer resonances: $3\nu_x=58$, $\nu_x+2\nu_y=58$, and 84 sextupoles located at vertical stations are used to control vertical chromaticity. The horizontal chromaticity sextupoles, located at horizontal stations, are presently used with one inch thick plastic spacers inserted between upper and lower coils. The harmonic content of these normal sextupole magnets and sextupoles with inserted plastic spacers with widths of 0.490", 0.520", 0.765", 0.790", 1.01", and 1.188", has been measured. The harmonic amplitudes have been measured by Morgan coils with radii of 4.3066, 2.766, 2.390, and 1.510 cm. Table 1 shows the harmonic amplitudes of the sextupole magnet for different spacer widths.

The measured integrated magnetic fields of the first ten harmonics (excluding the 16 pole as the Morgan probes do not have coils for this pole) with respect to the sextupole field strength at one inch off the center for the sextupole magnet without spacers and with 0.490", 0.790", and 1.050" plastic spacers are presented in Table 2.

Chromaticity sextupoles control the dependence of the tune of the machine on the momentum of the beam. They provide the desired chromaticity value by cancelling a constant value of the remnant sextupole in the main dipoles and by matching the time varying values of the natural chromaticity, eddy current sextupole field ($\propto B'/B$) etc., during parabola of the ramp. Due to the first need for chromaticity control at 'high' field during the coalescing process in the last machine run currents through the sextupole coils had to be much higher than the designed values. A dependence of the integrated sextupole field strength versus the coil excitation current has been checked with the Hall and with the

Morgan probes. The Hall probe measurements when the current was changed up to 40 amps as well as the Morgan probe measurements up to 19 amps showed no saturation and a linear function of the field with negligible deviations.

TABLE 1

SPACER WIDTH IN INCHES	SEXTUPOLE AMPLT. IN $\text{kGm/m}^2/\text{A}$	STANDARD DEVIATION	NUMBER OF MEASUREMENTS
0.000	4.664	0.017	17
0.490	3.870	0.016	5
0.520	3.793	0.009	6
0.765	3.447	0.014	11
0.790	3.361	0.015	5
1.010	3.025	0.012	25
1.050	2.927	----	2
1.188	2.790	----	2

As the current through the coils during the parabola changes in all harmonic measurements of the sextupole magnet with and without spacers, the harmonics have been measured for different current excitations in a range between 2-16 A. All values of the harmonic components, with the dipole as the only exception, have not shown noticeable differences for different current excitations. A current dependence of the field strength, of the noticeable normal components of harmonics of the sextupole magnet with an inserted 1.01" plastic spacer at 1" off the center, is presented in Fig. 1.

The field strength of the dipole harmonic divided by the sextupole field strength has shown a difference at low currents because the measured remnant dipole is higher than the remnant sextupole, which will be shown later.

A very small misalignment of the measuring probe produces in the first order calculation the next harmonic component with a smaller harmonic number. For example, if the probe is 0.2 mm off the central position the quadrupole harmonic within the sextupole magnet will be 7.9% of the sextupole field strength at one inch off the center. After corrections for the misaligned probe (see Appendix 1) the measured harmonic components of the sextupole magnet without spacers are schematically presented in Fig. 2, while Fig. 3, Fig. 4, and Fig. 5 present harmonic components of the sextupole magnet with 0.490", 0.790", and 1.050" plastic

spacers respectively.

The gradients of the sextupole magnets with different spacer width had been measured earlier with the Hall and Rawson probes (see TM-543) by B.A. Prichard. A one inch plastic spacer had been chosen to match the gradient of the B1 magnets. It had been shown (TM-543) that the remnant field of the B1 and B2 magnets contains higher order multipoles added to the dominating sextupole component. By adding a one inch plastic spacer in the horizontal plane of the sextupole magnet the negative decapole harmonic (see Table 2) distorts the field and makes an S shape for the gradient curve. Using the measured results of the harmonic amplitudes the integrated magnetic field $B_y \cdot L_{eff}$ and the gradient along the x-axis have been reconstructed. Fig. 6 presents the gradient of the sextupole magnet without and with 0.490", 0.790", and 1.050" thick plastic spacers.

TABLE 2

SPACER WIDTH IN INCHES		MEASURED INTEGRATED FIELD OF HARMONICS DIVIDED BY THE FIELD OF THE NORMAL SEXTUPOLE HARMONIC AT 1 INCH OFF IN THE CENTER IN PERCENTS							
		DIPOLE	QUAD.	OCTUP.	DECAP.	12 PL.	14 PL.	18 PL.	20 PL.
0.0	N	-2.40	1.70	.160	.370	.082	.840	-.349	.212
	S	.079	-2.92	.019	.044	-.091	-.040	.004	-.030
.490	N	-37.5	-1.24	-.305	-4.16	.057	.757	-.339	-.018
	S	-2.36	-1.32	.044	.029	-.026	-.080	.051	.021
.790	N	-35.4	-.971	-.507	-4.60	.001	.426	-.373	.108
	S	-3.55	-5.98	.185	-.005	-.133	.028	.059	-.350
1.01	N	-18.2	2.72	-.817	-4.83	.059	.459	-.540	.042
	S	.508	-4.71	.286	.054	-.003	.076	-.027	.006

(where "N" and "S" are shorthands for the "normal" and "skew" harmonic, respectively).

MAGNETIC FIELD DEPENDENCE ON THE COIL EXCITATION CURRENT FOR SOME OF THE NORMAL HARMONIC COMPONENTS

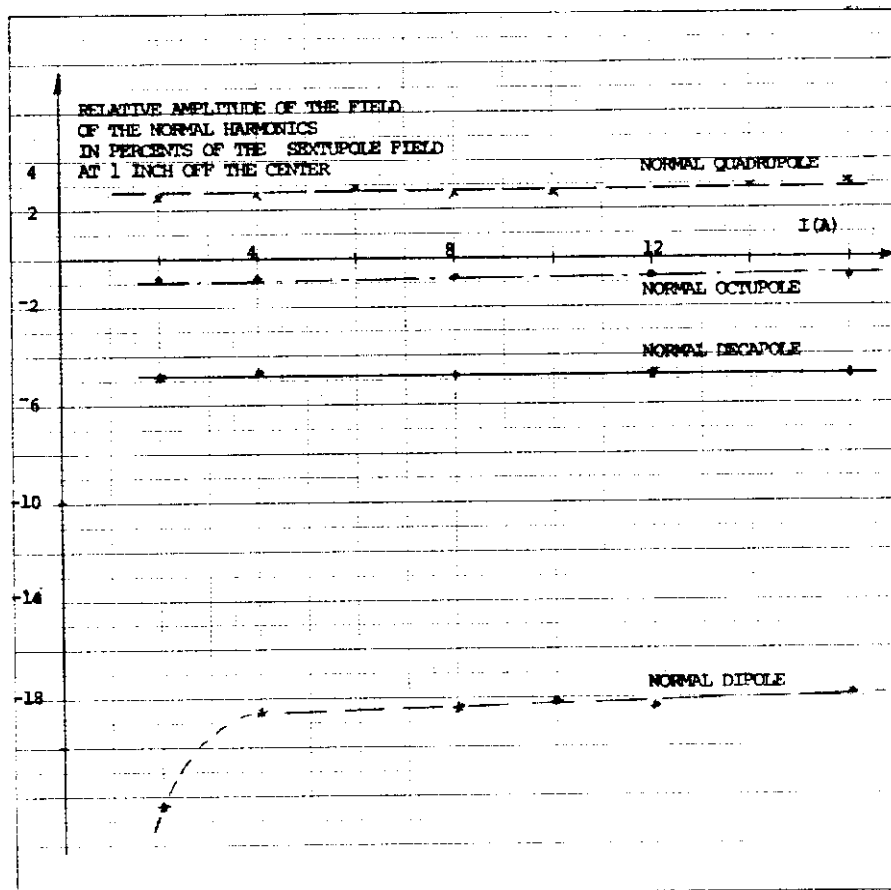
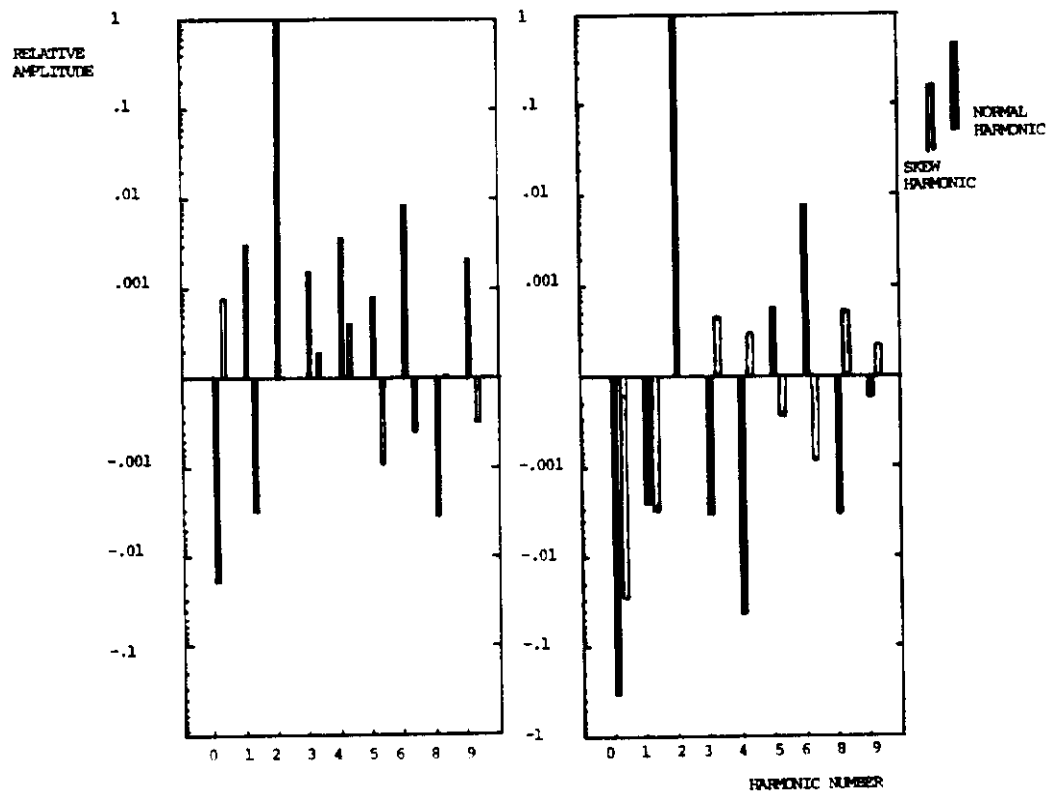


FIGURE 1

GRAPHIC PRESENTATION OF THE RELATIVE MAGNETIC FIELD
STRENGTH OF HARMONIC COMPONENTS WITH RESPECT TO THE
SEXTUPOLE FIELD STRENGTH AT 1 INCH OFF THE CENTER



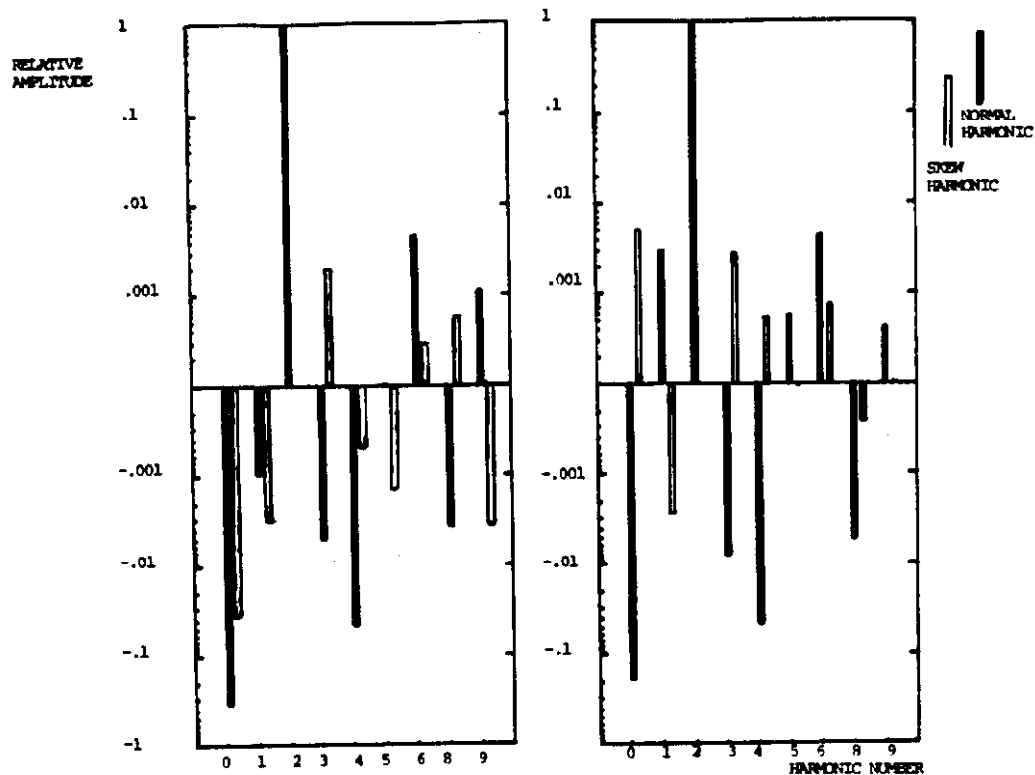
NORMAL SEXTUPOLE

FIGURE 2

SEXTUPOLE WITH
0.490" SPACER

FIGURE 3

GRAPHIC PRESENTATION OF THE RELATIVE MAGNETIC FIELD
STRENGTH OF THE HARMONIC COMPONENTS WITH RESPECT TO THE
SEXTUPOLE FIELD STRENGTH AT 1 INCH OFF THE CENTER



SEXTUPOLE WITH
0.790" SPACER

FIGURE 4

SEXTUPOLE WITH
1.01" SPACER

FIGURE 5

GRADIENT OF THE INTEGRATED FIELDS OF THE SEXTUPOLE WITH DIFFERENT SPACER WIDTHS

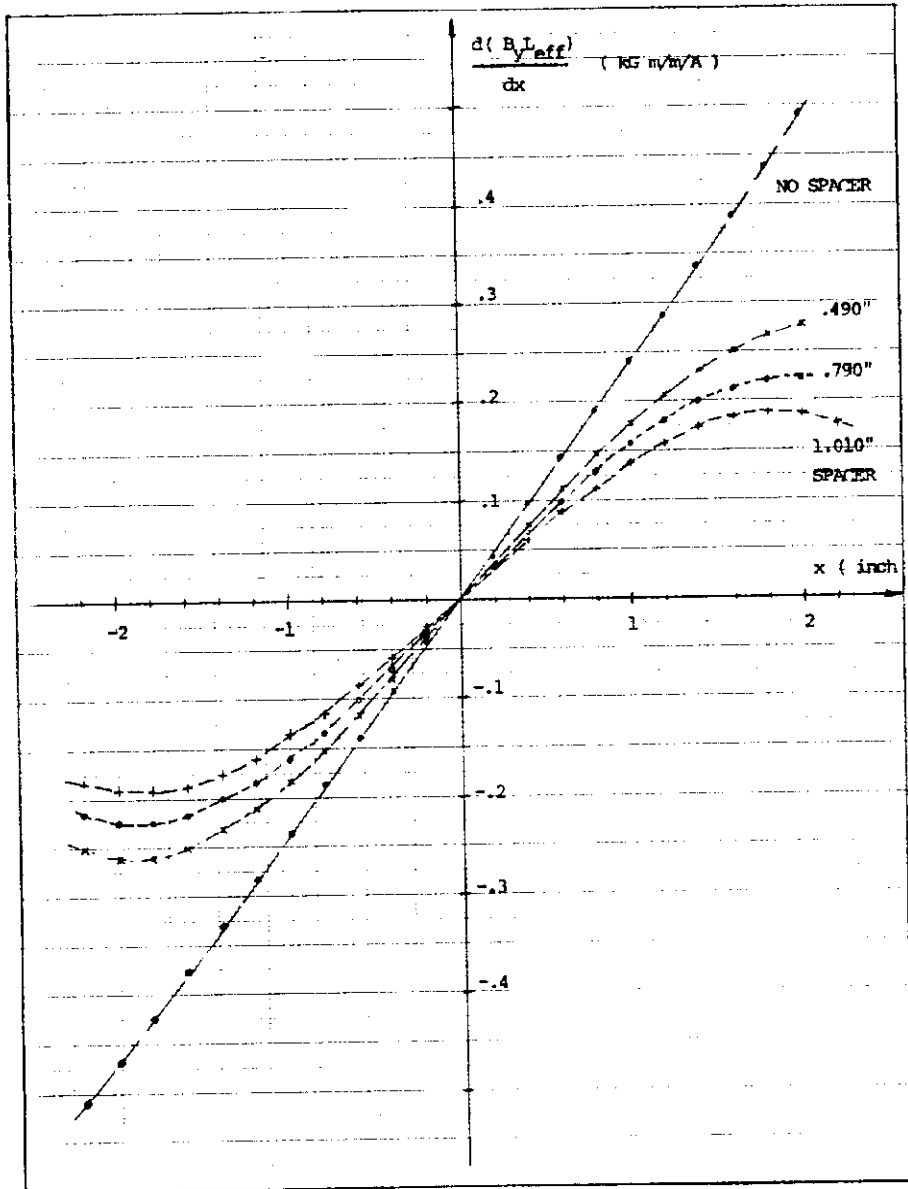


FIGURE 6

Slopes of the gradients (presented in Fig. 6) calculated with the least square method for the linear part of the gradients are presented in Table 3.

TABLE 3
SLOPE OF THE GRADIENTS

SPACER WIDTH IN INCHES	GRADIENT SLOPE IN $\text{kGm/m}^2/\text{A}$
0.000	9.310
0.490	7.460
0.790	6.603
1.010	5.769

The remnant fields of the sextupole magnet (with and without spacers) and the environment around the probes, measured for the sextupole and dipole harmonics, are presented in Table 4.

TABLE 4

THE INTEGRATED REMNANT FIELDS AT 1 INCH OFF THE CENTER IN Gm				
SPACER WIDTH	0.00	.490"	.790"	1.050"
SEXT. $b_2 \cdot L_{\text{eff}} \cdot r^2$.051	.049	.041	.039
DIPOLE $b_0 \cdot L_{\text{eff}}$.292	.245	.197	.194

Because of aperture reasons normal sextupole magnets in the Main Ring are designed with twofold instead of the usual threefold symmetry. Two central coils crossing the y-axis have 20 turns, while because of asymmetry the other four coils have 140 turns. It should be mentioned that in the present situation in the Main Ring the horizontal chromaticity sextupoles with inserted plastic spacers are used with the coils designed, as mentioned above, for the normal sextupoles with the same number of turns.

The high values of the dipole field relative to the sextupole, presented in Table 2, measured by Morgan probes with radii of 1.510, 2.390, and 2.766 cm, were consistent. The probes were aligned properly because the quadrupole harmonic measured small values. Suprisingly smaller values of $b_0/b_2 = -7.9\%$ of the dipole harmonic relative to the sextupole have been obtained by the probe with a much bigger radius of 4.3066 cm.

New measurements with the bottom and top central coils powered with a different current than the other four coils, for reasons mentioned above, have been performed. The bottom and top central coils were bypassed by two variable resistors. The total resistance of the powered coils connected in a series measured $1.6\ \Omega$. The sextupole magnet has been balanced in a few steps by changing the resistance of the resistors, connected parallel to the top and bottom coils, from $1.2\ \Omega$ down to $0.3\ \Omega$. The integrated fields of harmonics relative to the sextupole field strength at one inch off the axis are presented in Table 5. The integrated sextupole harmonic amplitude for the magnet with balanced coils, using a resistance of $0.3\ \Omega$, and with 0.988" plastic spacer measured $2.955\ \text{kG m/m}^2$.

TABLE 5

SEXTUPOLE MAGNET WITH 1 INCH PLASTIC SPACER
WITH BALANCED COILS

INTEGRATED FIELDS OF HARMONICS DIVIDED BY THE FIELD OF THE NORMAL SEXTUPOLE HARMONIC AT 1 INCH OFF THE CENTER IN PERCENTS DIPOLE QUAD. OCTUP. DECAP. 12 PL. 14 PL. 18 PL. 20 PL.								
NORMAL	-3.540	2.320	-0.157	-4.120	0.030	0.078	0.193	-0.015
SKEW	3.480	0.768	-0.058	-0.024	-0.002	0.154	0.069	0.010

One set of harmonic measurements has been done on the sextupole with inserted one inch thick iron spacers. The harmonic content and a value of the sextupole amplitude are presented in Table 6.

TABLE 6

SEXTUPOLE MAGNET WITH 1 INCH IRON SPACER

THE INTEGRATED SEXTUPOLE AMPLITUDE $b_2 \cdot L_{\text{eff}} / I(A) = 3.112 \text{ kGm/m}^2/A$
 THE INTEGRATED REMNANT FIELDS AT 1 INCH OFF THE CENTER
 SEXTUPOLE $b_2 \cdot L_{\text{eff}} \cdot r^2 = 0.069 \text{ Gm}$
 DIPOLE $b_0 \cdot L_{\text{eff}} = 0.235 \text{ Gm}$

MEASURED INTEGRATED FIELD OF HARMONICS DIVIDED BY THE
 FIELD OF THE NORMAL SEXTUPOLE HARMONIC AT 1 INCH OFF
 THE CENTER IN PERCENTS

DIPOLE QUAD. OCTUP. DECAP. 12 PL. 14 PL. 18 PL. 20 PL.

NORMAL	60.3	-1.78	.046	-3.38	-.063	-.027	-.079	-.291
SKEW	.221	1.64	-.121	.071	-.067	-.025	.075	-.006

The harmonic content of the sextupole magnet with a 1.050" inserted plastic spacer has been measured with the "tangential" probe (made for the main dipole magnetic measurements) for probe calibration purposes.

2. SKEW SEXTUPOLE MAGNETS

There are eighteen skew sextupoles located at stations 14, 17, and 22. They are used to compensate for the $3\nu_y=58$ and $2\nu_x+\nu_y=58$ resonances. The integrated amplitude of the skew sextupole strength and harmonic content has been measured by two Morgan probes with radii of 2.39 and 2.766 cm. The integrated amplitude of the skew sextupole has shown a linear dependence on the coil excitation current. The excitation current was changed from 0-19 A. The remnant integrated skew sextupole field at 1 inch off the center was:

$$a_2 \cdot L_{\text{eff}} \cdot r^2 = 0.034 \text{ Gm},$$

while a mean value of the integrated skew sextupole amplitude, measured with the probe with the radius of 2.766 cm from 9 measurements, was:

$$a_2 L_{\text{eff}} / I(A) = 3.585 \text{ kGm/m}^2/A,$$

with the standard deviation of 0.006.

The harmonic content of the skew sextupole is presented in Table 7.

TABLE 7

INTEGRATED FIELD OF THE HARMONICS IN THE SKEW SEXTUPOLE
RELATIVE TO THE SKEW SEXTUPOLE FIELD AT 1 INCH OFF THE
CENTER IN PERCENTS

HARMONICS	DIPOLE	QUAD.	OCTUP.	DECAP.	12 PL.	14 PL.	18 PL.	20 PL.
NORMAL	-4.25	-.741	-.027	.177	.097	.046	-.007	-.003
SKEW	21.9	.078	.110	-.308	.003	-.772	.130	.480

Integrated magnetic field of harmonic amplitudes relative to the skew sextupole field at 1 inch off the center are presented graphically in Fig. 7 .

GRAPHIC PRESENTATION OF THE INTEGRATED FIELD
OF THE HARMONIC COMPONENTS RELATIVE TO THE
SKEW SEXTUPOLE FIELD AT 1 INCH OFF THE CENTER

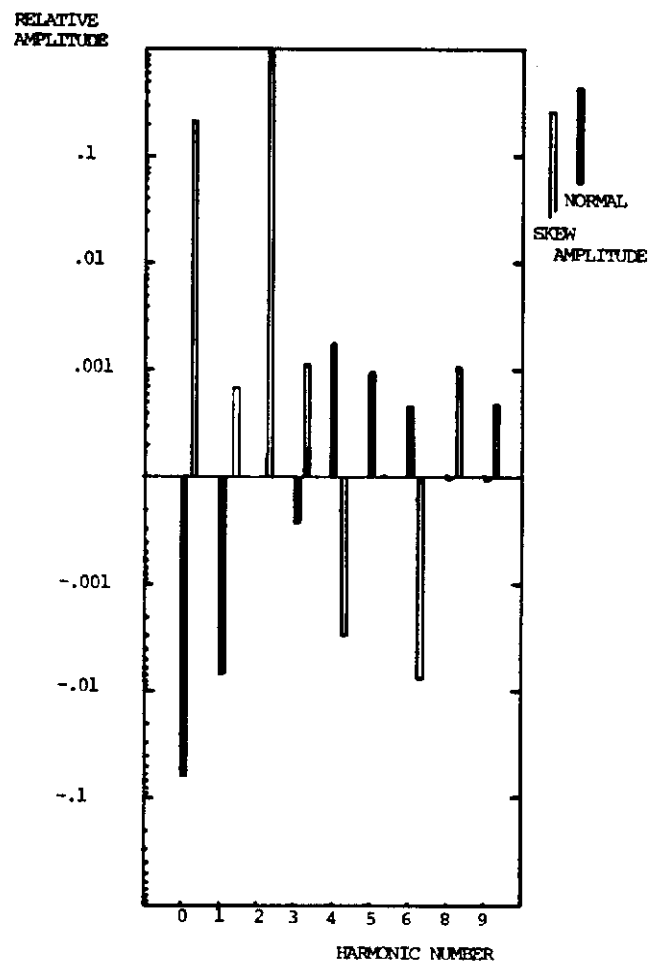


FIGURE 7

3. CHROMATICITY OCTUPOLE MAGNETS

The function of the thirty trim octupoles located at horizontal stations 17, 22, 28, 36, and 42 and fortyeight trim octupoles located at vertical stations 21, 23, 25, 27, 33, 35, 37, and 39 is to provide horizontal and vertical chromaticity correction rather than to correct any fourth-integer resonances. The octupole magnet has been measured by the Morgan probe with a radius of 2.766 cm. The current dependence of the integrated octupole amplitude was linear with a small value of the integrated remnant octupole field at 1 inch off the center :

$$b_3 * L_{eff} * r^3 = 0.0305 \text{ Gm},$$

while a mean value of the integrated octupole amplitude obtained from 9 measurements was:

$$b_3 * L_{eff} / I(A) = 27.921 \text{ kGm/m}^3/A,$$

with the standard deviation of 0.323. The harmonic content has been measured for current excitations of 2, 4, 6, 8, and 10 A. The current dependence of the harmonic components relative to the octupole as in the case of the sextupole magnet has shown straight lines except for a significant change of the dipole harmonic at 2 and 4 amps. This can easily be explained again by the higher remnant dipole field of the magnet (with additional influence of the environment) with respect to the low value of the remnant octupole field.

Table 8 shows the integrated fields of the harmonic components relative to the octupole field at 1" off the center.

The amplitude of the sextupole harmonic relative to the octupole at 1 inch off the center in a first set of measurements showed a relatively high value of 6%. Because the probe misalignment within the octupole magnet induces lower harmonics with more effect than in the case with other correction magnets an experiment was performed where the probe was intentionally misaligned by 0.5 cm off the center. The integrated field of the sextupole harmonic at 1 inch off the center measured 55.8% of the field of the octupole harmonic. A calculated value for the distance of misalignment using measured amplitudes of the sextupole and octupole harmonics is 0.425 cm. A graphic presentation of the integrated fields of harmonics relative to the octupole field at 1 inch off the center is presented in Fig. 8.

TABLE 8

INTEGRATED FIELD OF HARMONICS RELATIVE TO THE OCTUPOLE FIELD
AT 1 INCH OFF THE CENTER IN PERCENTS

HARM.	DIPOLE	QUAD.	SEXT.	DECAP.	12 PL.	14 PL.	18 PL.	20 PL.
NORMAL	-.470	-.075	-.760	-.099	.087	-.140	.052	-.099
SKEW	.297	-.092	.777	.269	-.156	-.168	-.103	-.269

GRAPHIC PRESENTATION OF THE INTEGRATED FIELD
OF THE HARMONIC COMPONENTS RELATIVE TO THE
OCTUPOLE FIELD AT 1 INCH OFF THE CENTER

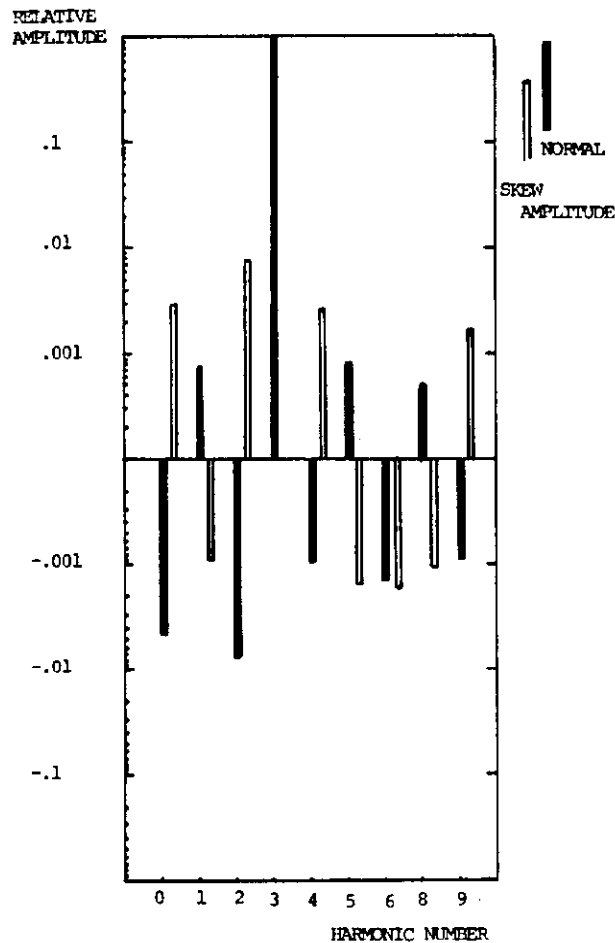


FIGURE 8

4. TRIM QUADRUPOLE MAGNETS

Twenty-four quadrupoles located at stations 36, 39, 42, and 45 are used to compensate for the $2\nu_x=39$ and $2\nu_y=39$ resonances. Harmonic measurements of the trim quadrupole have been performed by the use of the Morgan probes with a radius of 4.3066 cm and by the "tangential probe" for the purpose of calibrating it. The quadrupole harmonic has been measured with a current through the coils from 0-6 A with the integrated remnant quadrupole field at 1 inch off the center :

$$b_1 L_{\text{eff}} * r = 0.385 \text{ Gm.}$$

The quadrupole harmonic has shown a small deviation from the linear dependence on the current excitation. Values of the integrated quadrupole harmonic changed from 2.530 up to 2.574 kG/A for a current through the coils from 2 up to 6 A. The mean value of the integrated quadrupole harmonic was calculated as:

$$b_1 * L_{\text{eff}} / I(A) = 0.2551 \text{ kGm/m/A}$$

Magnetic measurements on a main ring trim quadrupole with a different method had been reported earlier in TM-927. Using the magnetic effective length of 34.85 cm from this TM for the 6 A excitation, the gradient is 4.432 kG/m.

Harmonic components have been measured with the excitation currents of 2, 4, and 6 A. It should be mentioned that all the harmonic coils of this probe have shown a much higher signal to noise ratio with respect to the other Morgan probes due to its larger radius. All harmonics except the dipole harmonic have shown a high linear dependence on the excitation current. The total relative integrated dipole field including the normal and skew components with respect to the quadrupole field at 1 inch off the center has shown values from 1.466% at the excitation of 2 A, down to 0.444% at 4 A excitation. The integrated field of different harmonics relative to the quadrupole field at 1 inch off the center are presented in Table 9, while Fig. 9 presents graphically the relative harmonic field at 1 inch off the axis.

TABLE 9

INTEGRATED FIELD OF THE HARMONIC AMPLITUDES RELATIVE TO THE
QUADRUPOLE FIELD AT 1 INCH OFF THE CENTER IN PERCENTS

HARM.	DIPOLE	SEXT.	OCTUP.	DECAP.	12 PL.	14 PL.	18 PL.	20 PL.
NORMAL	.187	-.173	.407	.051	-.168	-.009	.003	-.005
SKEW	-.403	-.017	.036	.015	-.013	-.005	.0001	-.001

GRAPHIC PRESENTATION OF THE INTEGRATED FIELD OF THE
HARMONIC COMPONENTS RELATIVE TO THE QUADRUPOLE FIELD
AT 1 INCH OFF THE CENTER

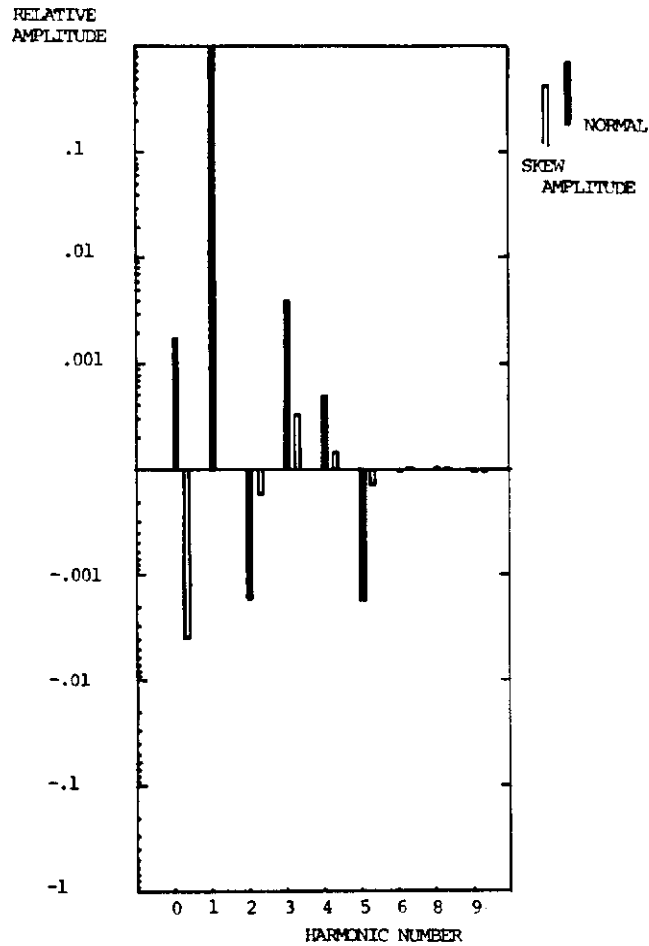


FIGURE 9

5. SKEW QUADRUPOLE MAGNET

The skew quadrupoles are used to compensate for the skew quadrupole imperfections in the guide field which drive the diagonal coupling resonance $\nu_x = \nu_y$. Eighteen skew quadrupoles are located at stations 27, 37, and 43.

For the magnetic measurements of the skew quadrupole magnet Morgan probes with radii of 2.390 and 2.766 cm have been used. The skew quadrupole harmonic amplitude dependence on the coil excitation current has shown a linear dependence for the measured range between 0-15 A. Signal differences for the all excitation currents were within the experimental error. The mean value of the integrated skew quadrupole amplitude obtained from 11 measurements taken by a probe with a 2.766 cm radius was:

$$a_2 \cdot L_{\text{eff}} / I(A) = 7.506 \cdot 10^{-2} \text{ kGm/m/A},$$

with the standard deviation of $0.061 \cdot 10^{-2}$. It is interesting to note that the other Morgan probe with a radius of 2.390 cm for the amplitude of the skew quadrupole measured a very close value of $7.501 \cdot 10^{-2} \text{ kGm/m/A}$.

The integrated amplitude of the remnant skew quadrupole field at 1 inch off the center was:

$$a_1 \cdot L_{\text{eff}} \cdot r = 0.034 \text{ Gm}.$$

The harmonic components have been measured by the 2.766 radius Morgan probe at coil excitation currents of 4 and 8 A, while with the 2.390 cm radius Morgan probe the current was 8 A. There was no significant change in the amplitude of harmonics at two different currents. The measured phase angle and amplitude of the dipole harmonic showed a vertical misalignment of 1.6 mm of the probe with respect to the magnetic field center. The integrated field of harmonics relative to the skew quadrupole field at 1 inch off the center is presented in Table 10. The relative harmonic amplitudes are presented graphically in Fig. 10.

TABLE 10

INTEGRATED FIELD OF THE HARMONIC AMPLITUDES
RELATIVE TO THE FIELD OF THE SKEW QUADRUPOLE
AT 1 INCH OFF THE CENTER IN PERCENTS

HARM.	DIPOLE	SEXTUP.	OCTUP.	DECAP.	12 PL.	14 PL.	18 PL.	20 PL.
NORMAL	-6.21	-.649	-.146	-.083	.018	.221	-.204	.053
SKEW	-.737	-.036	-.754	.013	.252	.021	.073	-.079

GRAPHIC PRESENTATION OF THE INTEGRATED FIELD
OF THE HARMONIC COMPONENTS RELATIVE TO THE
SKEW QUADRUPOLE FIELD AT 1 INCH OFF THE CENTER

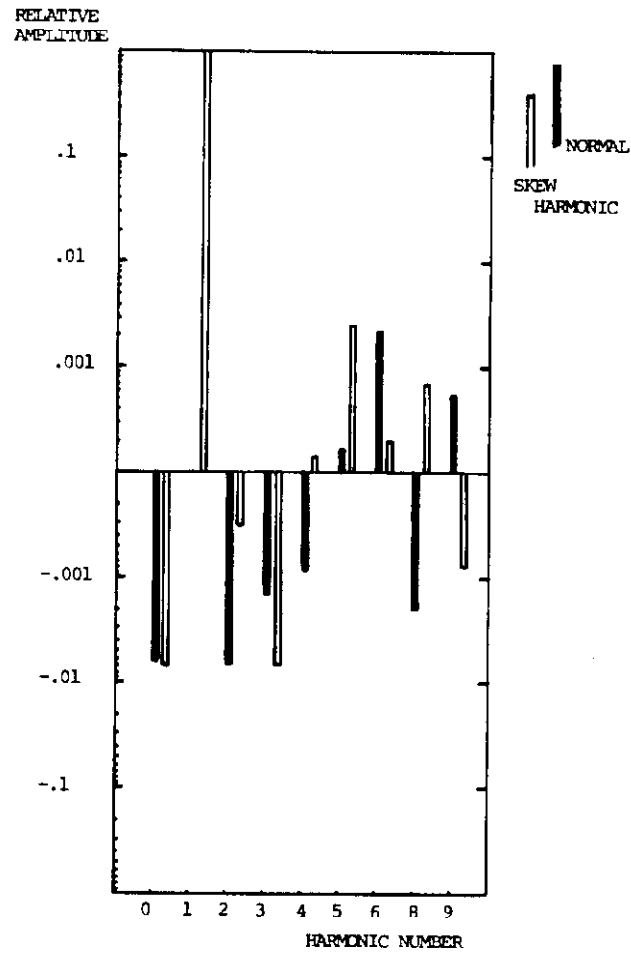


FIGURE 10

6. HORIZONTAL ADJUSTMENT DIPOLES

There are 108 horizontal adjustment dipoles located at horizontal stations with six magnets located at the '49' stations. Eighteen horizontal dipoles located at stations 11, 48, and 49 are stronger and with a wider aperture.

6.1 STRONGER HORIZONTAL DIPOLES

For the magnetic measurements of the stronger horizontal dipoles with 2*5 inch² aperture and 10 inch length the Morgan probe and the "tangential" coil with radii of 2.39 cm and 1.5 cm, respectively, have been used. The dipole integrated field strength has been measured with the coil excitation current up to 7 A. The integrated remnant field at 1 inch off the axis was:

$$b_0 * L_{eff} = 1.364 \text{ Gm}$$

The dipole field has shown a linear dependence on the current excitation. The mean value of the integrated field obtained from 10 measurements for current through the coils of 1, 2, 5, 6, and 7 A was:

$$b_0 * L_{eff} / I(A) = 5.858 * 10^{-2} \text{ kGm/A},$$

with the standard deviation of $0.014 * 10^{-2}$.

The harmonic content has been measured for the excitation current of 4 A. The integrated fields of harmonics relative to the dipole field strength at 1 inch off the axis are presented in Table 11. Fig. 11 is a graphic presentation of the field of harmonic amplitudes relative to the dipole integrated field at 1 inch off the axis.

TABLE 11

INTEGRATED MAGNETIC FIELD OF HARMONICS RELATIVE
TO THE DIPOLE FIELD OF THE STRONGER HORIZONTAL DIPOLE
AT 1 INCH OFF THE CENTER IN PERCENTS

HARM.	QUADR.	SEXT.	OCTUP.	DECAP.	12 PL.	14 PL.	18 PL.	20 PL.
NORMAL	.0022	-.6720	.0034	-.0248	-.0066	-.0271	-.0180	.0067
SKEW	-.0494	.0117	.0095	.0047	.0003	.0036	.0028	-.0057

GRAPHIC PRESENTATION OF THE INTEGRATED FIELD
 OF THE HARMONIC COMPONENTS OF THE STRONGER
 HORIZONTAL ADJUSTMENT DIPOLE RELATIVE TO THE
 DIPOLE FIELD AT 1 INCH OFF THE CENTER

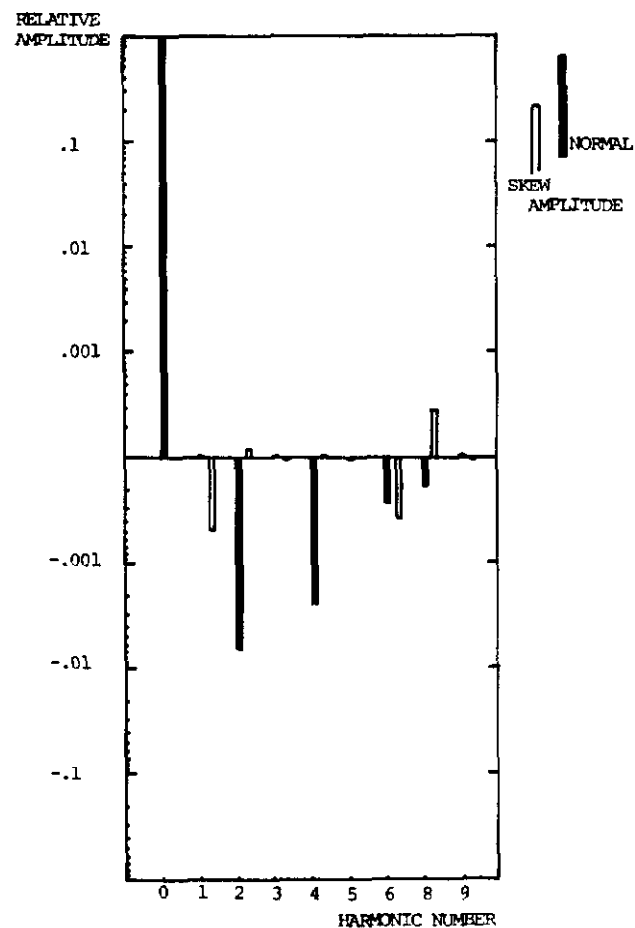


FIGURE 11

6.2 REGULAR HORIZONTAL DIPOLES

The magnetic measurements of the weaker horizontal dipoles with a smaller gap, with an aperture of 1.8×5 inch² and a length of 10 inches have been performed with a Morgan probe with a 1.510 cm radius and with the "tangential" coil with a 1.50 cm radius to calibrate the latter. Two horizontal magnets whose coils have the same number of turns but different end shape showed very similar magnetic properties. The current dependence of the dipole harmonic of both magnets has shown a linear dependence on the current excitations measured up to 10 A.

A mean value of the integrated dipole field obtained from 10 measurements for the horizontal dipole with molded coil ends (M) was:

$$b_0(M) \cdot L_{\text{eff}} / I(A) = 3.475 \cdot 10^{-2} \text{ kGm/A},$$

with the standard deviation of $0.012 \cdot 10^{-2}$; while the other horizontal dipole (N) showed a value from 10 measurements:

$$b_0(N) \cdot L_{\text{eff}} / I(A) = 3.405 \cdot 10^{-2} \text{ kGm/A},$$

with the standard deviation of $.1035 \cdot 10^{-2}$.

It should be mentioned that both kinds of dipole have shown slightly smaller values of the integrated dipole field at lower current excitations. For example for the dipole with molded coil ends this amplitude was:

$$b_0(2A) \cdot L_{\text{eff}} / I(A) = 3.453 \cdot 10^{-2} \text{ kGm/A},$$

and for the other kind of regular horizontal dipole:

$$b_0(2A) \cdot L_{\text{eff}} / I(A) = 3.361 \cdot 10^{-2} \text{ kGm/A}.$$

The integrated remnant dipole field at 1 inch off the center has shown the same values of:

$$b_0 \cdot L_{\text{eff}} \text{ rem} = 1.414 \text{ Gm},$$

for both types of dipoles.

The harmonic components of the weaker horizontal dipoles have been measured with a current excitation of 6 A, and have shown very similar values for both types of magnets. The integrated fields of the harmonics relative to the dipole field at 1 inch off the center are presented in Table 12, while Fig. 12 is their graphic presentation.

TABLE 12

INTEGRATED FIELD OF HARMONICS IN THE HORIZONTAL
DIPOLE RELATIVE TO THE DIPOLE FIELD AT 1 INCH
OFF THE CENTER IN PERCENTS

HARM.	QUADR.	SEXT.	OCTUP.	DECAP.	12 PL.	14 PL.	18 PL.	20 PL.
NORMAL	-.0346	-.1920	.0154	.0565	.0153	.0469	.0522	-.0057
SKEW	-.0550	-.0196	.0685	-.0577	-.1170	-.0985	.0190	.0146

GRAPHIC PRESENTATION OF THE INTEGRATED FIELD
OF THE HARMONICS IN THE HORIZONTAL DIPOLE
RELATIVE TO THE DIPOLE FIELD AT 1 INCH OFF CENTER

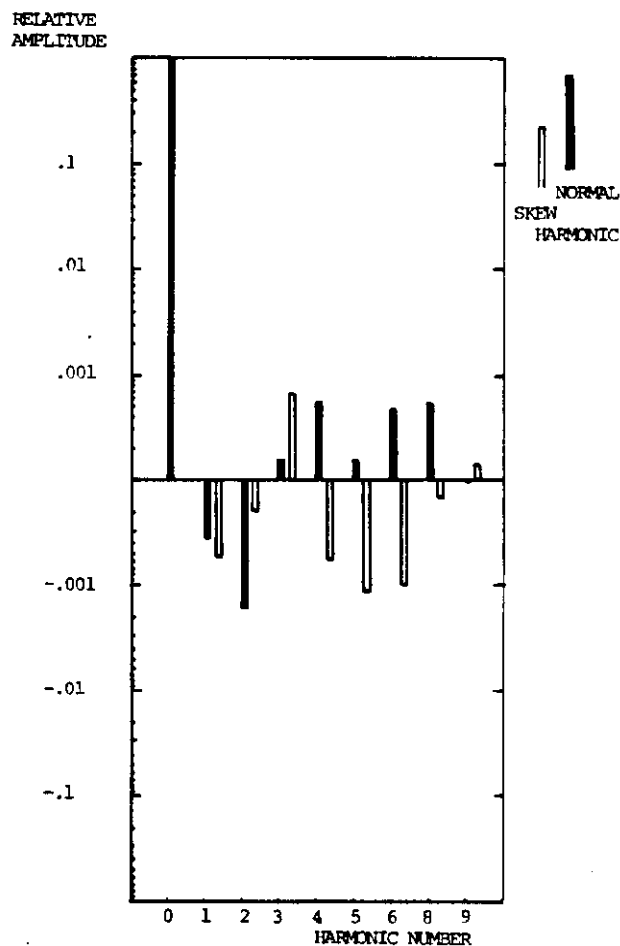


FIGURE 12

7. VERTICAL ADJUSTMENT MAGNETS

Hundred and eight vertical (skew) adjustment magnets are located at the vertical focusing stations including six magnets located at the '11' stations. Vertical adjustment magnets at stations 49 and 11 have an inserted 1 inch iron spacer in the central vertical plane.

The magnetic measurements of the skew dipoles have been taken with the Morgan probe with a radius of 2.766 cm.

7.1 REGULAR SKEW DIPOLE

The magnetic field strength dependence on the coil excitation current measured at excitations from 0-9 A has shown a linear characteristic. The integrated remnant skew dipole field at 1 inch off the center was:

$$a_0 \cdot L_{\text{eff}} \text{ rem} = 1.285 \text{ Gm.}$$

A mean value of the integrated skew dipole field obtained from 11 measurements was:

$$a_0 \cdot L_{\text{eff}} / I(A) = 2.166 \cdot 10^{-2} \text{ kGm/A,}$$

with the standard deviation of $0.0073 \cdot 10^{-2}$. The low current excitations have shown slightly lower values of the integrated dipole field (less than 0.5%). For example for the 2 A excitation the skew dipole field was $a_0 \cdot L_{\text{eff}} = 2.155 \cdot 10^{-2} \text{ kGm/A}$. The current dependence becomes very linear for coil excitation currents higher than 4 A.

The harmonic content of the skew dipole magnet measured at 3 A and 6 A currents has not shown a significant difference. The integrated magnetic fields of harmonic components relative to the skew dipole field at 1 inch off the center are presented in Table 13 for the 3 A excitation, while Fig. 13 is their graphic presentation.

TABLE 13

INTEGRATED MAGNETIC FIELD OF HARMONICS IN THE
SKEW DIPOLE RELATIVE TO THE SKEW DIPOLE FIELD
AT 1 INCH OFF THE CENTER IN PERCENTS

HARM.	QUADR.	SEXTUP.	OCTUP.	DECAP.	12 PL.	14 PL.	18 PL.	20 PL.
NORMAL	.161	-.196	.0149	.142	-.026	-.001	.062	-.007
SKEW	-.187	.722	-.249	-.587	.041	.004	-.062	-.014

GRAPHIC PRESENTATION OF THE INTEGRATED FIELD
OF THE HARMONICS IN THE SKEW DIPOLE RELATIVE
TO THE SKEW DIPOLE FIELD AT 1 INCH OFF CENTER

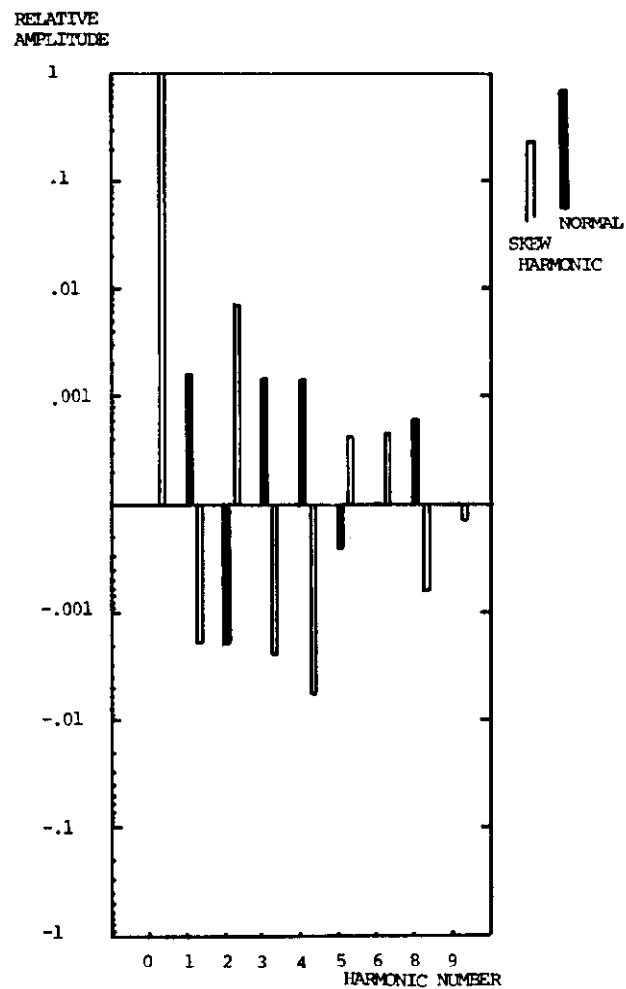


FIGURE 13

7.2 SKEW DIPOLE WITH 1 INCH IRON SPACER

The amplitude of the skew dipole has been measured at current excitations between 0-9 A. The integrated remnant skew dipole field at 1 inch off the center has shown a value of:

$$a_0 \cdot L_{eff} = 1.074 \text{ Gm.}$$

From the 7 measurements the mean value of the integrated dipole, which has shown a linear characteristic dependence on the current coil excitations was:

$$a_0 \cdot L_{eff} / I(A) = 1.680 \cdot 10^{-2} \text{ kGm/A,}$$

with a standard deviation of $0.006 \cdot 10^{-2}$. At low current excitations the amplitude of the skew dipole had slightly lower values. For example at 3 A current excitation the skew dipole was:

$$a_0(3A) \cdot L_{eff} / I(A) = 1.666 \cdot 10^{-2} \text{ kGm/A.}$$

The integrated remnant skew dipole field at 1 inch off the center was:

$$a_0 \cdot L_{eff} = 0.745 \text{ Gm.}$$

The harmonic content has been measured at current excitations of 2, 3, and 6 A. Amplitudes of the quadrupole, sextupole, octupole, decapole, and 12 pole harmonics differed markedly from the background signals. The values of the field of the harmonics relative to the skew dipole field have shown no observable change at different current excitations; they are presented in Table 14 for a current excitation of 3 A, while Fig. 14 is their graphic presentation. It should be noted thatt the 1 inch iron spacer significantly raised the sextupole and decapole harmonics with respect to the magnet without the spacer.

TABLE 14

INTEGRATED FIELD OF THE HARMONICS IN THE SKEW DIPOLE
WITH 1 INCH IRON SPACER RELATIVE TO THE SKEW DIPOLE
FIELD AT 1 INCH OFF THE CENTER IN PERCENTS

HARM.	QUADR.	SEXTUP.	OCTUP.	DECAP.	12 PL.	14 PL.	18 PL.	20 PL.
NORMAL	-.881	-.0022	.2880	.0226	-.0615	-.0005	-.0087	.0057
SKEW	-.0286	-6.160	.0791	-1.410	-.0312	.0021	-.0062	-.0003

INTEGRATED FIELD OF THE HARMONICS IN THE SKEW DIPOLE
WITH 1 INCH IRON SPACER RELATIVE TO THE SKEW
DIPOLE FIELD AT 1 INCH OFF THE CENTER

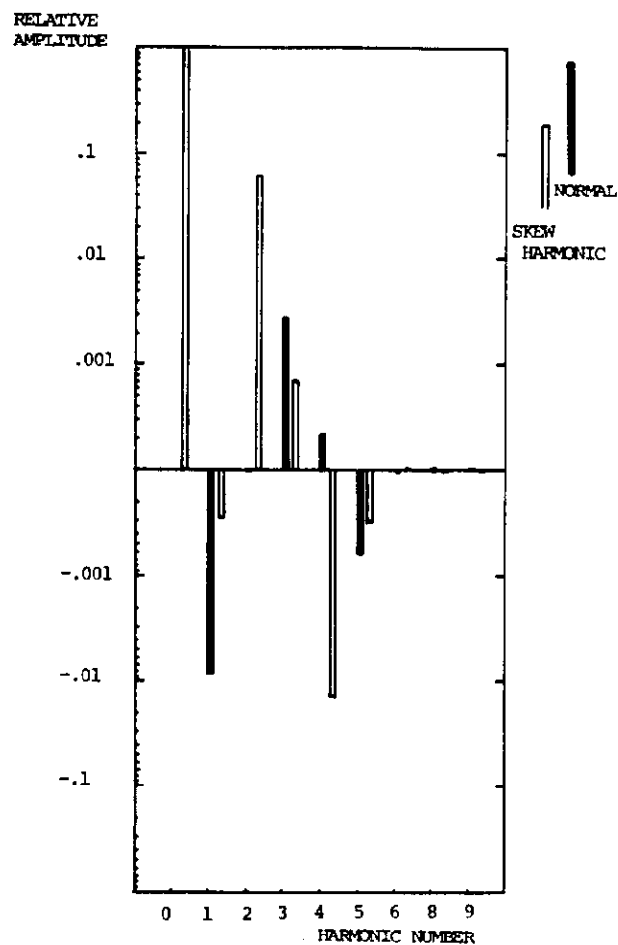


FIGURE 14

APPENDIX 1

1. Basic Formulae and Conventions

The region of interest does not include electric currents so the magnetic scalar potential ϕ_m is best for treatment. The Laplace equation must be satisfied:

$$\nabla^2 \phi_m = 0 \quad \dots\dots\dots(1)$$

where the magnetic induction field is:

$$\vec{B} = - \mu_0 \nabla \phi_m \quad \dots\dots\dots(2)$$

All correction elements are cylindrically symmetric so the same coordinate system is the most suitable. The solution of the Laplace equation (1) is:

$$\phi_m(r, \theta) = \phi_0 + \sum_{k=1}^{\infty} r^k (a_k \cos k\theta + b_k \sin k\theta) \dots\dots\dots(3)$$

For the cylindrical coordinate system the "r" and the "θ" components of the magnetic induction field are:

$$B_r(r, \theta) = -\mu_0 (\nabla \phi_m)_r = -\mu_0 \partial \phi / \partial r \quad \dots\dots\dots(4)$$

$$B_\theta(r, \theta) = -\mu_0 (\nabla \phi_m)_\theta = -\mu_0 r^{-1} \partial \phi / \partial \theta \quad \dots\dots\dots(5)$$

The equations (4) and (5) can be written as:

$$B_r(r, \theta) = -\mu_0 \sum_{k=1}^{\infty} k r^{k-1} (a_k \cos k\theta + b_k \sin k\theta) \dots\dots(4)$$

$$B_\theta(r, \theta) = -\mu_0 \sum_{k=1}^{\infty} k r^{k-1} (-a_k \sin k\theta + b_k \cos k\theta) \dots\dots(5)$$

where a_k and b_k are the skew and normal components, respectively, of the magnetic induction field. A convention used in the accelerator division of Fermilab is:

$$B_r(r, \theta) = \sum_{k=0}^{\infty} r^k [a_k' \cos (k+1)\theta + b_k' \sin (k+1)\theta] \dots(4)$$

$$B_{\theta}(r, \theta) = \sum_{k=0}^{\infty} r^k [-a_k' \sin (k+1)\theta + b_k' \cos (k+1)\theta] \dots (5)$$

where a_k' and b_k' include differences between two kinds of presentation. Appendix 2 contains the connection between the complex and real notations.

A vector of the magnetic induction field B can be projected to the x and y -axis. The projections B_x and B_y (avoiding further the apostrophe over a_k and b_k) are:

$$B_x = \sum_{k=0}^{\infty} r^k (a_k \cos k\theta + b_k \sin k\theta) \dots \dots \dots (6)$$

$$B_y = \sum_{k=0}^{\infty} r^k (-a_k \sin k\theta + b_k \cos k\theta) \dots \dots \dots (7)$$

The other convention used is that the magnetic induction field B_y is POSITIVE for the normal magnets across the x -axis ($\theta=0$).

1.1 Morgan Probe Formulae

The electromotive force ϵ induced at one moment in the coil of the Morgan probe crossing the magnetic field lines is:

$$\epsilon_j = -d\Phi/dt = - d/dt \int_S \vec{B} \cdot d\vec{S} = \int_L (\vec{v} \times \vec{B}) \cdot d\vec{l} \dots (8)$$

where Φ is the magnetic flux, dS the elemental surface, dl the elemental part of the coil crossing the field, and v is the speed of the coil crossing the field. A positive sign of the electromotive force ϵ coincides with the z -axis direction and is connected to the integrator (see Fig. 15).

$$\epsilon_j = -\int_0^{L_{eff}} v B_r(r, \theta) dl = -\omega \int_0^{L_{eff}} r B_r(r, \theta) dl = -L_{eff} \omega r B_r(r, \theta)$$

where $v = ds/dt = r d\theta/dt = r \omega$, and by expressing the field:

$$\epsilon_j = -L_{eff} \omega \sum_{k=0}^{\infty} r^k [a_k \cos (k+1)\theta + b_k \sin (k+1)\theta] \dots (8)$$

when a harmonic component with a harmonic number m is measured with the Morgan probe where the number of coils is $2N$, where N is equal to the harmonic number m , then the total signal of the probe is a simple summation of all signals from the coils as:

$$\epsilon_{\text{tot}} = \sum_{j=1}^{2N} \epsilon_j \quad \dots\dots\dots (9)$$

1.1.2 Magnetic Flux Formulae for the Morgan Probe

By definition the differential flux through an elementary surface dS which occurs by a sweep of the coil is:

$$d\Phi = \vec{B} \cdot \vec{dS} \quad \dots\dots\dots (10)$$

where $\vec{dS} = ds \times d\vec{l}$, where ds is a differential move of the coil $ds = r d\theta$, while $d\vec{l}$ is the coil element which is positive when it coincides with the z -axis direction. At one moment all coils of the Morgan probe sweep the same elemental surface:

$$d\vec{S} = r_0 (-1)^j r d\vec{l} d\theta \quad \dots\dots\dots (11)$$

passing through different magnetic induction field lines giving for the total differential flux :

$$d\Phi = r d\vec{l} d\theta \{ B_r(\theta) - B_r(\theta + \pi/N) + B_r(\theta + 2\pi/N) - \dots - B_r[\theta + (2N-1)\pi/N] \}$$

$$d\Phi = \sum_{j=0}^{2N-1} (-1)^j B_r(r + j\pi/N) r d\vec{l} d\theta \quad \dots\dots\dots (10)$$

Using the equation (4) for the projection of the magnetic induction field on the " r " axis $B_r(r, \theta)$ the differential flux can be written as:

$$d\Phi = \sum_{j=0}^{2N-1} (-1)^j \sum_{k=0}^{\infty} r^{k+1} [a_k \cos(k+1)(\theta + j\pi/N) + b_k \sin(k+1)(\theta + j\pi/N)] d\vec{l} d\theta$$

The total flux is the integral of $d\Phi$:

$$d\Phi = \int d\Phi = L_{\text{eff}} \sum_{k=0}^{\infty} (k+1)^{-1} r^{k+1} \sum_{j=0}^{2N-1} (-1)^j [a_k \sin(k+1)(\theta+j\pi/N) - b_k \cos(k+1)(\theta+j\pi/N)] \dots (11)$$

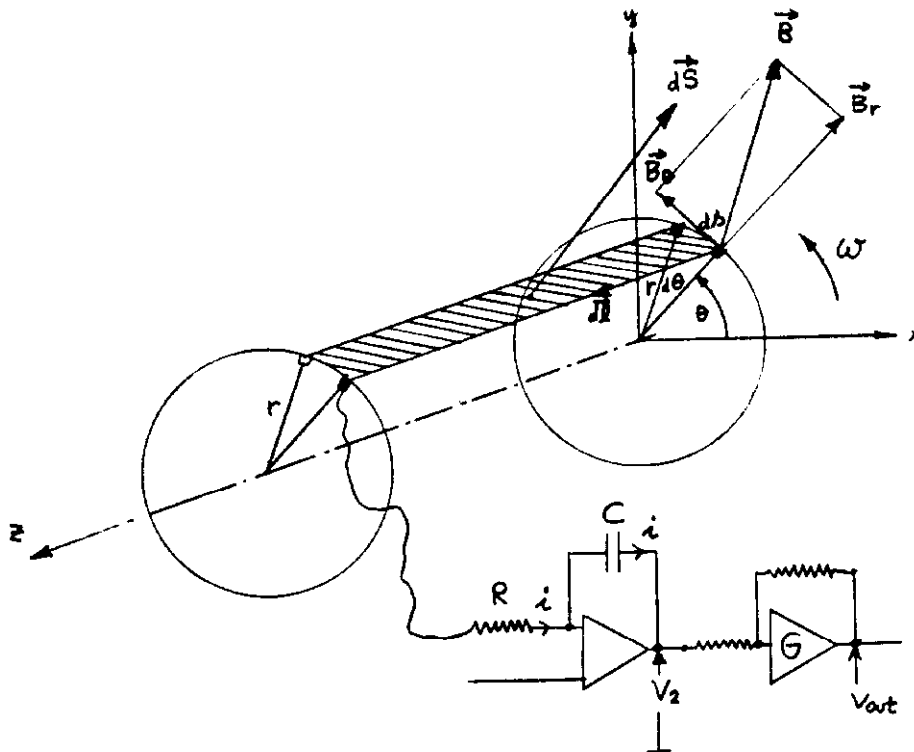


FIGURE 15

When:

$$k/N = 2\lambda \quad \text{the sum is:} \quad \sum_{j=0}^{2N-1} (-1)^j = 0 \quad \text{where } \lambda=1,2,3,4\dots,$$

while for:

$$k/N = 2\lambda-1 \quad \text{the sum is:} \quad \sum_{j=0}^{2N-1} (-1)^{2j+1} = -2N ,$$

and the total flux is :

$$\Phi = -2N L_{\text{eff}} \sum_{k=0}^{\infty} (k+1)^{-1} r^{k+1} [a_k \sin(k+1)\theta - b_k \cos(k+1)\theta] \quad \dots\dots\dots(12)$$

The harmonic amplitudes a_k and b_k can be presented in the complex form (see Appendix 2) as:

$$\tilde{C}_k = b_k + i a_k = C_k (\cos \chi_k + i \sin \chi_k)$$

The normal and skew amplitudes are connected with the complex constant C_k with:

$$a_k = C_k \sin \chi_k \text{ and the normal amplitude } b_k = C_k \cos \chi_k$$

The equation (12) can be written as:

$$\Phi = 2N L_{\text{eff}} \sum_{k=0}^{\infty} (k+1) r^{k+1} C_k \cos [(k+1)\theta + \chi_k] \quad \dots(13)$$

Fig. 15 shows that the output voltage can be found from:

$$\epsilon^{\text{tot}} = (R+r_c) \cdot i \quad \text{where } i = \epsilon^{\text{tot}} / (R+r_c) \quad \dots\dots\dots(14)$$

where r_c is the total resistance of the coils, while R is the resistor at the input of the integrator.

$$V_2 = -V_c, \quad V_c = C^{-1} \int i \, dt = (r_c+R)^{-1} C^{-1} \int \epsilon^{\text{tot}} \, dt \quad \dots\dots(15)$$

$$V_{\text{out}} = -G V_2 = G V_c = G(r_c+R)^{-1} C^{-1} \int \epsilon^{\text{tot}} \, dt \quad \dots(16)$$

where the V_c is a voltage on a capacitor of the integrator, while C is the capacitance, V_2 is the input voltage to the amplifier with the gain G .

As the magnetic flux is by definition the integral of the electromotive force:

$$\Phi = - \int \epsilon^{\text{tot}} \, dt = -[(r_c+R)C/G] \cdot V_{\text{out}} \quad \text{in } (T \, m^2) \text{ or } (V \, \text{sec}) \quad \dots\dots(17)$$

The measured signal V_{out} is Fourier analyzed by the fast Fourier transformation (FFT) and obtained as:

$$V_{out} = \sum_{k=0}^M V_k \cos[(k+1)\theta + \alpha_k] \quad \dots(18)$$

From the equations (17) and (18) one can write the identity:

$$2N L_{eff} \sum_{k=0}^{\infty} (k+1)^{-1} r^{k+1} C_k \cos[(k+1)\chi_k] = -(r_c+R)C/G * \sum_{k=0}^M V_k \cos[(k+1)\theta + \alpha_k]$$

The measured amplitudes of harmonic components are:

$$C_k L_{eff} = - [(r_c+R)C/2N*G] * [(k+1)/r^{k+1}] * V_k \quad k=0,1,2\dots$$

so the dipole amplitude is C_0 , the quadrupole is C_1 , and so on. The minus sign can be omitted if one adds π angle to the phase identity:

$$\chi_k = \alpha_k + \pi$$

The phases of harmonic components are measured relative to the phase of the main harmonic of the magnet which is partially defined bellow.

1.2 Phase angle definition

The phase angle is defined as an angle between a new position of the poles of a magnet with respect to the poles' positions of the normal magnet. At the new position at the tip of the magnet pole, described in Fig. 16 as a pole S' , the magnetic induction field in the " θ " direction must be zero ($B_\theta=0$):

$$B_\theta(r, \theta) = \sum_{k=0}^{\infty} r^k [-a_k \sin(k+1)\theta + b_k \cos(k+1)\theta] = 0$$

or:

$$a_k \sin(k+1)\theta = b_k \cos(k+1)\theta$$

As one can see from Fig. 16:

$$\theta + \phi' = \pi/2(k+1), \quad (\text{where } k=0,1,2,3,\dots) \quad \dots(19)$$

One can write from the conditions above:

$$a_k/b_k = [\cos(k+1)(\pi/2k-\phi')]/[\sin(k+1)(\pi/2k-\phi')] = \tan(k+1)\phi'$$

By a simple comparison one can see that:

$$(k+1)\phi' = \chi_k,$$

and the harmonic amplitudes a_k and b_k can be found as:

$$a_k = C_k \sin(k+1)\phi' = C_k \sin \chi_k$$

$$b_k = C_k \cos(k+1)\phi' = C_k \cos \chi_k$$

It is easy to show that if the magnet is turned counterclockwise for an angle ϕ'' this relation is valid:

$$a_k/b_k = - \tan(k+1)\phi'',$$

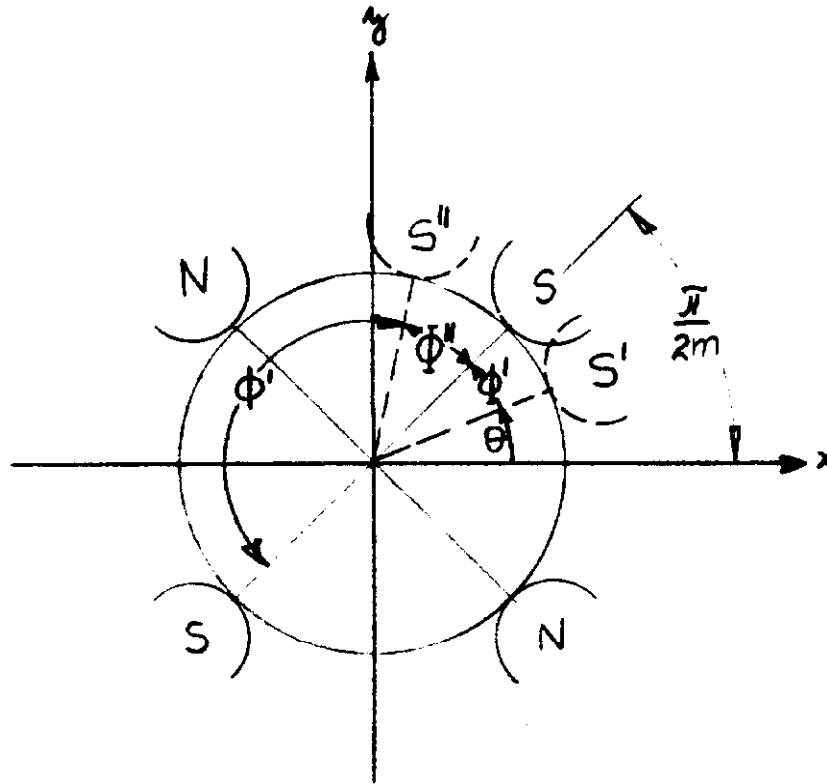


FIGURE 16

The result is the same if one uses an angle ϕ instead of using ϕ'' , where ϕ is defined as an angle between the new position of the magnet pole and the next position of the same kind of magnetic pole. The angle ϕ happens to be equal to ϕ' because:

$$\phi' + \phi'' = 2\pi/(k+1)$$

2. Correction of Results because of the Probe Misalignment

If the center of the probe is moved by a distance "a" off the center of the magnetic field, the new position of the probe is defined in the complex coordinate system as:

$$z' = z - a = r e^{i\theta} - a \quad \dots\dots\dots(20)$$

The magnetic induction field in complex notation in the "z" coordinate system (see for more details Appendix 2) is:

$$\tilde{B} = B_x + i B_y \quad \text{and} \quad \tilde{B}^* = \sum_{k=0}^{\infty} i C_k z^k$$

The magnetic field at new positions is:

$$\tilde{B}(z') = \sum_{k=0}^{\infty} i C_k (z')^k = \sum_{k=0}^{\infty} i C_k (r e^{i\theta} - a)^k = \sum_{k=0}^{\infty} i C_k r^k e^{ik\theta} (1 - ar^{-1} e^{i\theta})^k \quad \dots\dots(21)$$

One can use the binomial expansion for the small x:

$$(1-x)^m = 1 - mx + (1/2)m(m-1)x^2 + \dots + (1/n!)m(m-1)(m-2)\dots(m-n+1) x^n + \dots \quad \dots(22)$$

A harmonic component of the magnetic field "p" can be approximated using the expressions above as:

$$\tilde{B}_p \simeq i C_p r^p e^{ip\theta} - i a p C_p r^{p-1} e^{i(p-1)\theta} \quad \dots(23)$$

Instead of measuring the p-pole harmonic with an amplitude C_p one measures with the misaligned probe in the first approximation another harmonic with a harmonic number smaller by one.

Comparing the measured amplitudes of the expected harmonic "p" and the next unexpected "p-1" harmonic one finds the distance "a" for which the probe is misaligned as:

$$a = 1/p * C_{p-1}/C_p \quad \dots(24)$$

3. Gradient of the Magnetic Field along the X-Axis

Using the Fermilab conventions $B_y(x,y)$ or $B_y(r,\theta)$ can be written as:

$$\tilde{B}_y^* = \text{Im}(\tilde{B}), \text{ where the } \tilde{B} = \sum_{k=0}^{\infty} i C_k z^k, \text{ where } C_k = b_k + ia_k$$

The gradient of B_y along the x-axis is:

$$\partial B_y / \partial x = \text{Im} \left[\sum_{k=1}^{\infty} k i C_k (x + iy)^{k-1} \right] \quad \dots(25)$$

APPENDIX 2

Connection between the Complex and Real Notations**

The magnetic scalar potential can be presented with the complex notation as the imaginary part of the complex quantity $F(z)$ as:

$$\tilde{F} = A + iV \quad \text{where } z = x+iy = r e^{i\theta} \quad \dots(26)$$

where A is the only existing z-component of the vector \vec{A} perpendicular to the x-y plane.

** K.Halbach, Nuclear instr.& Methods 78(1970) 185-198p

The components of the strength of the magnetic field \tilde{H} are defined as:

$$H_x = \partial A / \partial y = -\partial V / \partial x \quad \text{and} \quad H_y = -\partial A / \partial x = -\partial V / \partial y \quad \dots (27)$$

where $\tilde{H} = H_x + iH_y$ (amp-turns/m)

The complex quantity $F(z)$ can be expanded into a Taylor series in "z" as:

$$\tilde{F}(z) = \sum_{k=0}^{\infty} \tilde{C}_k z^k \quad \dots \dots \dots (28)$$

For the complex function $F(z)$ the derivatives with respect to x and y variables exist if the Cauchy-Riemann conditions are satisfied:

$$\partial A / \partial x = \partial V / \partial y \quad \text{and} \quad \partial A / \partial y = -\partial V / \partial x \quad \dots \dots \dots (29)$$

The derivative of the $F(z)$ is defined from the complex analyses as:

$$\begin{aligned} d\tilde{F}(z)/dz &= \partial A / \partial x + i\partial V / \partial x = \partial V / \partial y - i\partial A / \partial y = \partial A / \partial x - i\partial A / \partial y = \\ &= \partial V / \partial y + i\partial V / \partial x \quad \dots (30) \end{aligned}$$

$$i d\tilde{F}(z)/dz = -\partial V / \partial x + i\partial V / \partial y = H_x - iH_y$$

As the complex conjugate of \tilde{H} is:

$$\tilde{H}^* = H_x - iH_y ; \quad H_x = -\partial V / \partial x \quad \text{and} \quad H_y = -\partial V / \partial y$$

$$\tilde{H}^* = i d\tilde{F}(z)/dz \quad \dots \dots \dots (31)$$

$$d\tilde{F}(z)/dz = \sum_{k=0}^{\infty} k \tilde{C}_k z^{k-1} \quad \dots \dots \dots (32)$$

$$\tilde{H} = i \frac{dF(z)}{dz} = \sum_{k=1}^{\infty} i k \tilde{C}_k z^{k-1} \quad \dots\dots\dots(33)$$

If one defines $\tilde{C}_k = C_k \exp(i\chi_k) = C_k (\cos \chi_k + i \sin \chi_k) \dots(34)$

Or by writing the complex constant C_k as:

$$\tilde{C}_k = b_k + i a_k \quad ,$$

where a_k and b_k are the skew and normal amplitudes.

The projections of the strength of the magnetic field \tilde{H} on the x-y coordinates H_x and H_y can be found from:

$$\tilde{H} = H_x - i H_y = \sum_{k=1}^{\infty} i k (b_k - i a_k) z^{k-1}$$

As one can see this summation starts from $k=1$ which was changed in the accelerator division of Fermilab to the summation starting from $k=0$. This convention was earlier mentioned in Appendix 1. H_x and H_y are defined from the equation above as:

$$\begin{aligned} H_x &= - \sum_{k=1}^{\infty} k r^{k-1} [b_k \sin(k-1)\theta + a_k \cos(k-1)\theta] \\ H_y &= - \sum_{k=1}^{\infty} k r^{k-1} [b_k \cos(k-1)\theta - a_k \sin(k-1)\theta] \quad \dots(35) \end{aligned}$$

To express the projections of the magnetic field strength \tilde{H} on the θ - r coordinate system (see Fig. 17) one has to rotate the coordinate system x-y by an angle θ so that a new system will be:

$$z' = z e^{i\theta} \quad ,$$

and all complex variables, as for example $\tilde{H}(z)$, will be dependent on z' as:

$$\tilde{H}(z') = \tilde{H}(z) e^{i\theta} \quad ,$$

now the complex conjugate of \tilde{H} can be written as:

$$\tilde{H}^*(z') = \sum_{k=1}^{\infty} i^k (b_k - ia_k) r^{k-1} e^{i(k-1)\theta} e^{i\theta} \quad \dots\dots(36)$$

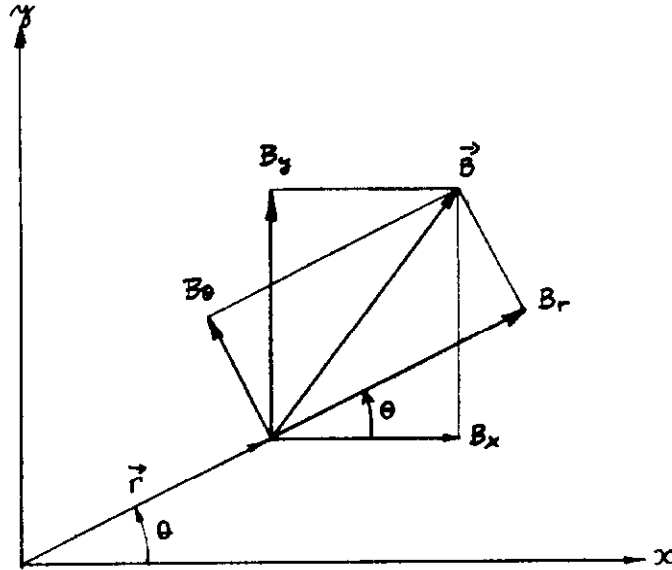


FIGURE 17

The rotation of the coordinate system z by an angle θ changes the components of the magnetic field intensity so that the real part of the complex conjugate of \tilde{H} becomes a projection in the "r" coordinate while the imaginary part of it, with a change of sign, defines the " θ " projection as:

$$H_r(r, \theta) = \text{Real} [\tilde{H}^*(z')] = - \sum_{k=1}^{\infty} k r^{k-1} (a_k \cos k\theta + b_k \sin k\theta) \quad \dots\dots(37)$$

$$H_\theta(r, \theta) = \text{Im} [\tilde{H}^*(z')] = - \sum_{k=1}^{\infty} k r^{k-1} (-a_k \sin k\theta + b_k \cos k\theta) \quad \dots\dots(38)$$